The Effect of Chitosan Type and Concentration on Physical Characteristics and Drug Release Behavior of Andrographolide-Chitosan Microparticles Prepared by Ionic Gelation – Freeze Drying

Proceedings of International Conference on Applied Pharmaceutical Sciences (ICoAPS) 2018

9 Pages
Posted: 11 Oct 2019
Last revised: 6 Dec 2019

Retno Sari (https://papers.ssrn.com/sol3/cf_dev/AbsByAuth.cfm?per_id=3757119)
Faculty of Pharmacy, Airlangga University

M.L.L. Sugiarto (https://papers.ssrn.com/sol3/cf_dev/AbsByAuth.cfm?per_id=3757224)
Airlangga University - Faculty of Pharmacy, Airlangga University

W. Amirah (https://papers.ssrn.com/sol3/cf_dev/AbsByAuth.cfm?per_id=3757226)
Airlangga University - Faculty of Pharmacy, Airlangga University

H. Yusuf (https://papers.ssrn.com/sol3/cf_dev/AbsByAuth.cfm?per_id=3757230)
Airlangga University - Faculty of Pharmacy, Airlangga University

Date Written: September 30, 2019

Abstract

Andrographolide is low in solubility and bioavailability, with short half-life (t1/2 = 1.5-2 hours), with chitosan micro-particles expected to improve its dissolution. Therefore, the objective of this research was to investigate the effect of chitosan concentration and the in vitro release of andrographolide from micro-particles prepared by ionic gelation using sodium tripolyphosphate (TPP) as cross-linker. Furthermore, the micro-particles used were prepared with two different concentration of chitosan namely 19 cPs and 50 cPs. The result showed that the micro-particles obtained were spherical in shape and heterogeneous in size, with Infrared spectra indicating ionic bonding between chitosan and TPP. The DTA thermogram and XRD diffractogram exhibited a change in crystal structure to a more amorphous form. The entrapment efficiency (EE) of andrographolide in micro-particles was about 78%, with no impact on the chitosan concentrations (19 cPs and 50 cPs) affected by EE. The kinetics released was followed by the Higuchi model in phosphate buffer, with pH 7 ± 0,05 higher than the andrographolide substance. It was investigated that andrographolide-chitosan micro-particles had the ability to enhance its dissolution rate.

Keywords: microparticle, andrographolide, chitosan, ionic gelation, drug release

19 References

1. S A Agnihotri, N N Mallikarjuna, T M Aminabhavi
   Recent advances on chitosan-based micro-and nanoparticles
   Journal of Controlled Release, volume 100, issue 1, p. 5 - 28
   Posted: 2004
   Crossref (https://doi.org/10.1016/j.jconrel.2004.08.010)

2. B Chellampillai, A P Pawar
   Improved bioavailability of orally administered andrographolide from ph-sensitive nanoparticles
   Drug metabolism pharmacokinetics, volume 35, issue 3-4, p. 123 - 129
   Posted: 2011

Crossref (https://doi.org/10.1007/s13318-010-0016-7)

3. P He, S S Davis, L Illum
Chitosan microspheres prepared by spray drying
International Journal of Pharmaceutics, volume 187, issue 1, p. 53 - 65
Posted: 1999
Crossref (https://doi.org/10.1016/s0378-5173(99)00125-8)

4. E M Hejjaji, A M Smith, G A Morris
Designing chitosan-tripolyphosphate microparticles with desired size for specific pharmaceutical or forensic applications
International Journal of Biological Macromolecules, volume 95, p. 564 - 573
Posted: 2016
Crossref (https://doi.org/10.1016/j.ijbiomac.2016.11.092)

Load more

Paper statistics

DOWNLOADS	26
ABSTRACT VIEWS	174

19 References

PlumX Metrics

(https://plu.mx/ssrn/a/?ssrn_id=3461443)

The effect of chitosan type and concentration on physical characteristics and drug release behavior of andrographolide-chitosan microparticles prepared by ionic gelation – freeze drying

R. Sari, M.L.L. Sugiarto, W. Amirah, H. Yusuf

Department of Pharmaceutics, Faculty of Pharmacy, Universitas Airlangga, Surabaya, Indonesia

*Corresponding author: R. Sari (retno-s@ff.unair.ac.id)

ABSTRACT: Andrographolide is low in solubility and bioavailability, with short half-life (t1/2 = 1.5-2 hours), with chitosan micro-particles expected to improve its dissolution. Therefore, the objective of this research was to investigate the effect of chitosan concentration and the in vitro release of andrographolide from micro-particles prepared by ionic gelation using sodium tripolyphosphate (TPP) as cross-linker. Furthermore, the micro-particles used were prepared with two different concentration of chitosan namely 19 cPs and 50 cPs. The result showed that the micro-particles obtained were spherical in shape and heterogeneous in size, with Infrared spectra indicating ionic bonding between chitosan and TPP. The DTA thermogram and XRD diffractogram exhibited a change in crystal structure to a more amorphous form. The entrapment efficiency (EE) of andrographolide in micro-particles was about 78%, with no impact on the chitosan concentrations (19 cPs and 50 cPs) affected by EE. The kinetics released was followed by the Higuchi model in phosphate buffer, with pH 7 ± 0,05 higher than the andrographolide substance. It was investigated that andrographolide-chitosan micro-particles had the ability to enhance its dissolution rate.

Keywords: microparticle, andrographolide, chitosan, ionic gelation, drug release

1. INTRODUCTION

Andrographis paniculata commonly referred to as sambiloto is a medicinal plant which is commonly grown in Asia and often used in the treatment of various diseases. Its main compound is Andrographolide which has a wide range of pharmacological effects such as anti-inflammatory, antidiarrheal, antiviral, antimalarial, anticancer, hepatoprotective, and immunostimulatory. However, despite its numerous benefits, andrographolide solubility in water is low, with high lipophilicity, and short half-life. Furthermore, it is rapidly absorbed, metabolized, and unstable at an extremely acidic or basic condition in the digestive tract. These characteristics, therefore, led to the drug's low bioavailability (Kanokwan & Nubuo, 2008; Panossian et al. 2011; Agnihotri et al. 2004; Jiang et al. 2014; Chellampillai & Pawar, 2011). However, one of the strategies used to improve its properties are particulate or solid particle dispersions of drug and polymeric matrix with its sizes in the range of 1µm - 1000µm (Agnihotri et al. 2004; Kumari et al. 2016; Rasenack & Müller, 2004).

Chitosan is a derivative of cationic polymer, which is easier to process from shrimp and crabs (Rinaudo, 2006). It has biocompatible, biodegradable, as well as non-toxic properties, and produced using non-toxic multivalent polyanion, tripolyphosphate (TPP) as a crosslinker. The formation of particles using ionic gelation technique is advantageous because the process is simple and easy, without the use of organic solvent and high temperature (Rampino et al. 2013). Its mechanism is formulated through electrostatic interaction between the positive charges of the amino group and the negative of TPP (Rampino et al. 2013). Microparticles are spontaneously formed when chitosan is sprayed into the TPP solution, with dry micrparticles obtained by the freeze-drying method. This process increases its stability by removing water from the dispersion to obtain the dry form by a sublimation process. It has the ability to improve the stability of active ingredient via barrier formed between the drug and the external environment, by enhancing the dissolution rate. While the control

and the release of insoluble drugs has the ability to extend the release time due to an enhancement in its half life (Rasenack & Müller, 2004; Sinha et al. 2004).

The concentration and viscosity of chitosan solution are some of the factors that tend to influence the formation of micro-particles. The higher the molecular weight, the higher its viscosity, thereby, leading to a relatively strong micro-particle formation, which interacts with the TPP using a spherical and smooth surface. The increasing polymer concentration also enhances its viscosity, followed by the formation of larger droplets, thereby, producing larger particles, which has the ability to increase absorption efficiency (Hejjaji et al. 2016; Agnihotri et. al. 2004; He et al. 1999).

The drug released from the microparticles is influenced by the number of crosslinkers', the polymer viscosity, and its molecular weight. This is inversely proportional to the crosslinking concentration, polymer's molecular weight and its amount, with the ability to enhance its amount in the microparticles (Sinha et al. 2004; Ko et al. 2002).

The release of kinetics model and dosage of drug comprises of certain mechanism, used to identify and transport it in order to obtain the appropriate drug concentration in the blood. The quantitative analysis method of drug is easily obtained using a mathematical approach such as the dependent model which comprises of order 0, order 1, Higuchi, Korsmeyer-Peppas, and Hixson-Crowell (Sinko & Yashveer, 2011; Malana & Rubab, 2013).

The research therefore aims to investigate the effect of chitosan concentration and its type on physical characteristics and drug release rate.

2. MATERIALS AND METHODS

2.1 Materials

Andrographolide (RD Health Ingredients Co., Ltd, China), chitosan 19 cPs (Biotech. Co. Ltd, Indonesia), chitosan 50 cPs (Biotech. Co. Ltd, Indonesia), sodium tripoliphosphate (Nacalai Technique, Japan), maltodextrine (SoriniAgro Asia Corporindo, Indonesia), acetic acid pro analysis, ethanol pro analysis, aquades, methanol pro analysis, and all other reagents used in this experiment were of analytical grade.

2.2 Methods

2.2.1 Microparticle preparation

According to Table 1, andrographolide was weighed and dissolved in ethanol, while Chitosan was dissolved in acetic acid solution with 1.5 times of its concentration obtained at 0.5% and 0.75%. This was followed by mixing as well as stirring andrographolide and chitosan solutions at 500 rpm which was obtained using a spray gun (0.6 mm nozzle diameter) at pH 5.0. It was further stirred continuously at 500 rpm for 30 minutes till 1000 rpm and centrifuged at 2500 rpm to separate the microparticles, which was followed by the dispersion of the supernatant with 5% maltodextrin solution using lyoprotectant and dried for 48 hours. The obtained dry particles were then evaluated.

Table 1. Andrographolide-chitosan microparticles composition.

Formula	Weight (mg)		
	Chitosan	TPP	Andrographolide
L0.5	250	1250	100
L0.75	375	1250	100
M0.5	250	1250	100
M0.75	375	1250	100

*L= 19 cPs chitosan; M= 50 cPs chitosan

2.2.2 Morphology evaluation

The size and surface morphology of the microparticles were observed in a holder and coated with gold-palladium prior to SEM Analysis using Scanning Electron Microscopy (SEM) (S50 Type 2017/12 inspect).

2.2.3 Fourier transform infrared (FTIR) analysis

The evaluation was performed to determine the interaction between andrographolide, chitosan and TPP. Approximately 2 mg of microparticle was mixed with 300 mg KBr, and compressed with a hydraulic press to form transparent pellets which were observed at a wavelength of 4000-400 cm^{-1} using Jasco FT-IR 5300.

2.2.4 X-ray diffraction analysis

The evaluation was carried out to determine the crystallinity structure of andrographolide change in chitosan microparticles. Samples were analyzed using a PRO analytical Diffractometer X'Pert at room temperature with the measurement conditions of X Kα light source, Cu target, Ni filter, 40 kV voltages, and 40 mA in the range 2Ø 5-40°.

2.2.5 Differential thermal analysis
Approximately 5 mg sample was placed in a crucible pan and examined at 50°C-250°C with a temperature increment of 10°C per minute using a Differential Thermal Analyzer (Mettler Toledo FP-65 DTA P-900 Thermal).

2.2.6 Redispersability evaluation
2 ml of distilled water was added to 50 mg of microparticles in the vial, and sonicated for 5 minutes, followed by the observation of the sedimentation process for 5, 30 and 60 minutes.

2.2.7 Andrographolide content and entrapment efficiency of microparticles
The andrographolide amount was determined spectrophotometrically by adding 5 ml of methanol to 10 mg microparticles, and sonicated for 15 minutes. The solution was filtered with a Ø 0.45 µm membrane and observed using UV-Vis spectrophotometer UH 5300 at the wavelength 225 nm. The drug content and entrapment efficiency were calculated using the equations below:

Drug content = (drug amount/particle weight) x 100%

Entrapment efficiency = (actual drug amount/theoritical drug amount) x 100% $Drug\ loading = \frac{drug\ amount}{particle\ weight} Drug\ loading = \frac{drug\ amount}{particle\ weight}$

2.2.8 In vitro release evaluation
The in vitro drug release test was carried out on phosphate buffer medium, pH 7.00 ± 0.05, with the microparticle weighing about 5 mg of andrographolide and then put into the medium. The tests were carried out on a shaker water bath with media volume of 50.0 ml, at 37 ± 0.50C. Furthermore, 2 mL of the sample was taken at the specified time for 5 hours and were analyzed using the UV-Vis spectrophotometer at a wavelength of 225 nm.

2.2.9 Release kinetic
To evaluate the andrographolide release kinetic from the chitosan microparticles, the released data were calculate by the following equations (Sinko & Yashveer, 2011; Malana & Rubab, 2013):
Zero order equation:

$$Q_t = Q_0 + k_{0t} \quad Q_t = Q_0 + k_{0\ t} Q_t = Q_0 + k_{0t}$$

where Q_t is the percentage of drug released at time (t) and k0 is the release rate constant.
First order equation:

$$Ln\ (100 - Q_t) = ln\ 100 - k_{1t}$$

Where k_1 is the first order release rate constant.
Higuchi equation:

$$Q_t = K_{H\ t}^{1/2}$$

K_H represents drug release constant for Higuchi
Korsmeyer-Peppas equation:

$$Q_t/Q_e = k_{KPt}^{n}$$

k_{KP} is the drug release constant for Korsmeyer-Peppas

3. RESULTS

3.1 Results and discussion

3.1.1 Morphology of microparticles
The results of SEM in Figure 1 showed a spherical particles for all formulas.

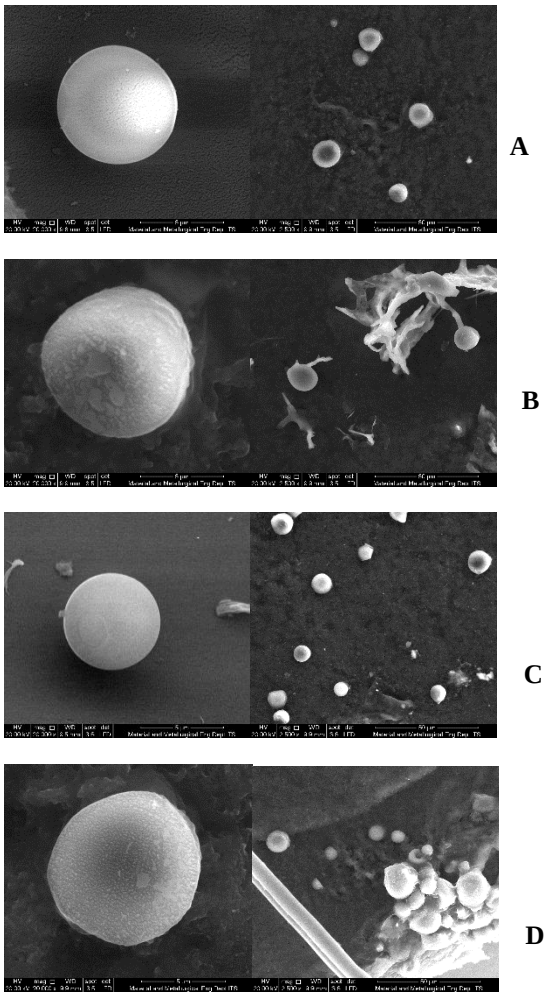

Figure 1. SEM micrographs of andrographolide-chitosan microparticles with different types and amounts of chitosan; (A) 19 cPs 0.5% , (B)19 cPs 0.75%, (C) 50 cPs 0.5%, (D) 50 cPs 0.75%. Left: 2500 x magnification, Right: 20.000 x magnification.

3.1.2 Infrared spectrum

In Figure 2, the Chitosan infrared spectra had a specific absorption at wave number 3444 cm^{-1} with OH and NH groups, using amide bond (-C=O) at 1654 cm^{-1}. While the microparticles system's spectra indicated the absorption band at 1654 cm^{-1} which disappeared, with the appearance of a new absorption at wave numbers between 1645 cm^{-1} and 1535 cm^{-1}.

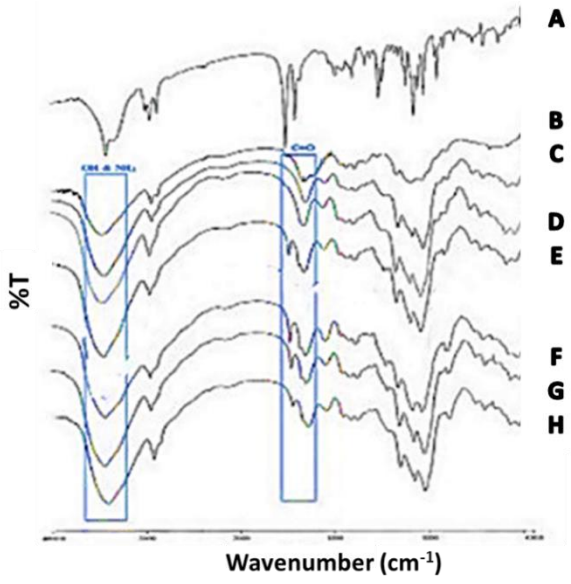

Figure 2. Infrared spectra of (A) Andrographolide, (B) Chitosan, unloaded chitosan microparticles: (C)19 cPs, (D)50 cPs, andrographolide-chitosan microparticles : (E)19 cPs 0.5% ,(F)19 cPs 0.75%, (G)50 cPs 0.5%, (H), 50 cPs 0.75%.

3.1.3 X-ray diffraction

In Figure 3, X-ray diffractogram of andrographolide showed a crystalline structure, while chitosan and all the microparticle formulas indicated an amorphous structure.

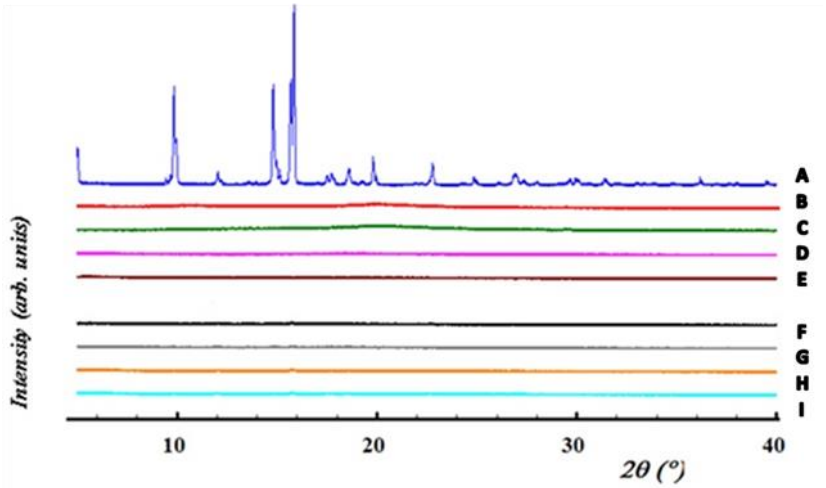

Figure 3. X-ray diffractogram of (A) Andrographolide, (B) 19 cps chitosan, (C) 50 cps chitosan, empty chitosan microparticles: (D) 19 cPs, (E) 50 cPs, andrographolide-chitosan microparticles with different types and amounts of chitosan : (F)19 cPs 0.5%, (G) 19 cPs 0.75%, (H), 50 cPs 0.5% , (I), 50 cPs 0.75%.

3.1.4 Differential thermal analysis (DTA)

DTA thermogram of the andrographolide-chitosan microparticle had a different thermogram profile with lower melting point compared to the thermogram of andrographolide as shown in Figure 4.

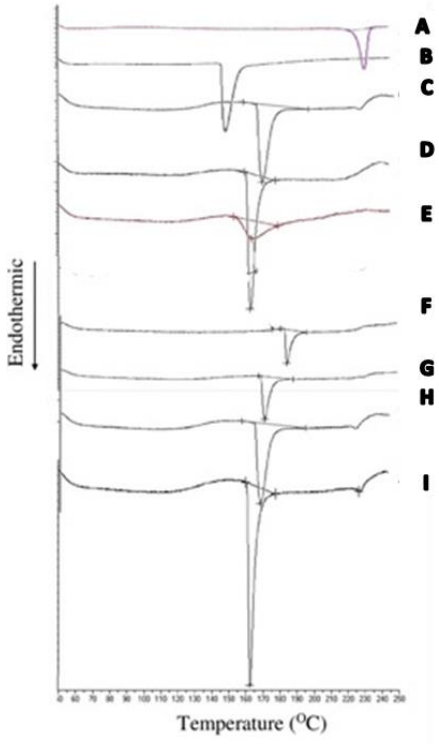

Figure 4. DTA Thermogram from (A) Andrographolide, (B) 19 cps Chitosan, (C) 50 cps chitosan, empty chitosan microparticles: (D) 19 cPs, (E) 50 cPs, andrographolide-chitosan microparticles with different types and number of chitosan (F)19 cPs 0.5%, (G) 19 cPs 0.75%, (H) 50 cPs 0.5%, (I) 50 cPs 0.75%.

3.1.5 Redispersability test

Figure 5 showed the redispersability of the andrographolide-chitosan microparticles in water.

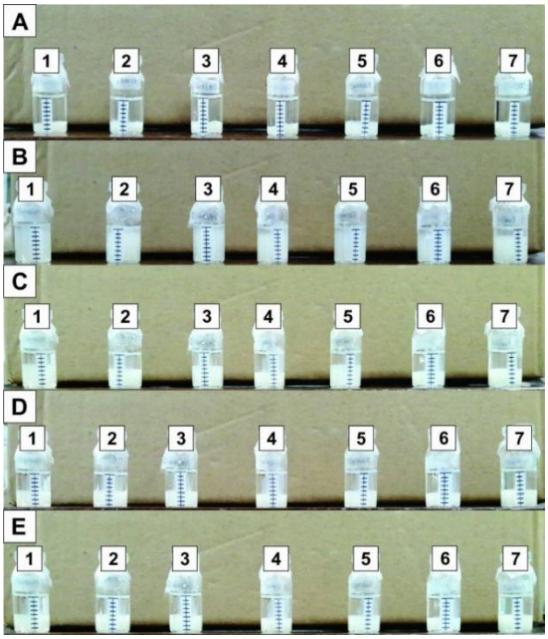

Figure 5. The redispersabilty test result of (1) chitosan 19 cps microparticles, (2) andrographolide (3) 19 cps 0.5%, (4) 19 cps 0.75%, (5) chitosan 50 cps microparticles and andrographolide (6) 50 cps 0.5%, and (7) 50 cps 0.75% at different times (A) before and after redispersion, (B) 0 minutes, (C) 5 minutes, (D) 30 minutes, and (E) 60 minutes.

3.1.6 Drug content and entrapment efficiency (EE) of microparticles

From the results of the andrographolide content evaluation, it showed that the 0.5% concentration of chitosan for both 19 cPs and 50 cPs had a higher drug content and EE compared to the 0.75%.(Table 2).

Table 2. Drug content and entrapment efficiency of andrographolide

Formula	Drug content (%)	Entrapment Efficiency (%)
L0.5	7.12 ± 0.03	78.30 ± 0.29
L0.75	5.07 ± 0.40	62.11 ± 2.56
M0.5	7.03 ± 0.09	77.37 ± 1.03
M0.75	6.44 ± 0.07	70.82 ± 0.77

3.1.7 In vitro drug release

The results of drug release evaluation showed that the andrographolide released in the phosphate buffer media, pH pH 7.00 ± 0.05 was higher (Figure 6). The release rate from the micro-particles confirmed that drug release was faster than the substance (Table 3).

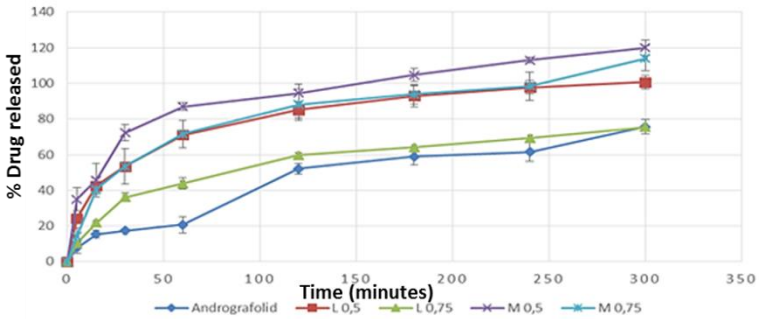

Figure 6: Andrographolide release profile from chitosan microparticles in phosphate buffer media (pH 7.00 ± 0.05).

Table 3. Drug released rate constants of andrographolide-chitosan microparticles.

Formula	Slope ± SE (%drug released/minute$^{1/2}$)
Andrographolide	4.2933 ± 0.4164
L0.5	7.7768 ± 0.3991
L0.75	5.5940 ± 0.2443
M0.5	8.7136 ± 0.3197
M0.75	8.4059 ± 1.0826

3.1.8 Release kinetics

The release kinetics was determined by calculating the data using the zero, and first orders, as well as the Higuchi and Korsmeyyer Peppas models as seen in Table 4. The chosen kinetic model was the highest value of the correlation coefficient (R^2).

Table 4. The release kinetics correlation coefficient (R^2) of the microparticles.

Formula	Zero Order	First Order	Higuchi	Korsmeyyer Peppas
L0.5	0.8857	0.6047	0.9836	0.9137
L0.75	0.9277	0.6883	0.9927	0.9619
M0.5	0.8326	0.5715	0.9570	0.8931
M0.75	0.9023	0.6529	0.9851	0.9486

4. DISCUSSION

4.1 Morphology of microparticles

Figure 1 showed that all microparticles had spherical shape, but 0.5% chitosan for both 19 cPs and 50 cPs gave more spherical shape and a smoother surface compared to those with higher chitosan concentration (0.75%). This was due to the increase in the type and amount capable of reducing its crosslinking density.

4.2 Infrared spectrum

In the infrared spectra of chitosan (Figure 2), there were a specific absorption at wave number 3444 cm^{-1} of -OH group and -NH group, also amide bond (-C=O) at 1654 cm^{-1}. Whereas the microparticle system indicated that the absorption band at wave number 1654 cm^{-1} disappeared and new absorption band appeared at wave numbers 1646 cm^{-1} and 1535 cm^{-1} at L0.5, 1645 cm^{-1} and 1536 cm^{-1} at L0.75, 1646.54 cm^{-1} and 1542.58 cm^{-1} at M0.5, as well as 1644.55 cm^{-1} and 1544.59 cm^{-1} at M0.75. The new absorption band indicated interaction between NH_3^+ ion of chitosan and $-P_3O_{10}^{5-}$ of TPP which proved a crosslinking bond between chitosan and TPP.

The amount and molecular weight of chitosan was related to the availability of NH_3^+ protonated from chitosan which interacted with $-P_3O_{10}^{5-}$ of TPP to crosslink. This interaction affects the microparticles characteristics such as morphology, particle size, drug encapsulation which further affect the drug release, bioavailability and effectiveness (Sonia & Sharma, 2011; Kumar et al. 2011; Sari et al. 2017).

4.3 X-ray diffraction analysis

From the X-ray diffractogram, the crystallinity of the solid sample is observed, with low solubility. Therefore as the drug's crystallinity altered the amorphous structure, it was advantageous to drug solubility. Since the amorphous form had higher solubility than the crystalline, its bioavailability was enhanced (Murphy & Rabel, 2008). In Figure 3, X-ray diffractogram of andrographolide showed a crystalline structure, whereas chitosan indicated an amorphous structure. The diffractograms andrographolide-chitosan microparticle formulas, and the peak of Andografolid were still visible at an angle of 2θ 9.8°, 12°, 14.8°, 15.7° with small intensity. While its diffractogram did not show sharp diffraction peaks from andrographolide, which showed that andrographolide has undergone a change in crystalline structure due to the recrystallization barriers of crosslinked chitosan (Sari et al. 2017).

4.4 Differential thermal analysis

In Figure 4, it is seen that the endothermic peak of particles differ with andrographolide and chitosan. The melting point of andrographolide was 239.2˚C and became lower up to 50˚C at the formation of microparticles. The endothermic peak of the chitosan was around 170˚C to 180˚C and this showed that andrographolide has been entrapped in the system in different forms of structure. In accordance with the X-ray diffractogram (Figure 3), the change of drug's crystallinity became less crystalline or amorphous structure capable of lowering the melting point.

4.5 Redispersability test

Redispersability test showed that the five andrographolide-chitosan microparticles were easily dispersed as observed by the formation of fine particles such as opalescent aqueous suspension slowly sedimented for 5 minutes. However, after 60 minutes, it remained higher than the powder before it redispersed the particles with fine sediments easily dispersed.

4.6 Drug content and entrapment efficiency of microparticles

The composition and preparation methods used in this study led to the drug entrapment efficiency (EE) of 77%, which was higher compared to the previous researches, were they were dried with spray drying methods and the EE was about 30% (Sari et al. 2017). Freeze drying method could minimize drug loss during the drying process. From the results, it was known that an increase in the amount of chitosan led to a decrease in the efficiency of andrographolide entrapment. These results were due to the less availability of $-P_3O_{10}^{5-}$ and TPP which interacted with excess $-NH_3$ as the chitosan concentration increased. Conversely, as the crosslinking degree increased, it inhibits the drug entrapment process as shown in particles L0.75. However, the different types of chitosan (19 cPs and 50 cPs) gave no difference in the microparticle's EE.

4.7 In vitro drug release

The drug release profile from chitosan microparticles in phosphate buffer pH 7.00 ± 0.05 showed an enhanced formation of the dissolved particles. These results supported the X-ray and DTA analysis's results from the previous section. In addition, the slope value demonstrated that the L0.75 particles had the slowest rate, with 50 cPs each. Ko et al. (2002) stated that chitosan concentration caused the formation of a strong wall due to its interaction with crosslinking. The high bond density between chitosan and TPP caused a decrease in swelling ability, thereby, inhibiting drug diffusion at a slower rate (Ko et al. 2002).

4.8 Release kinetics

The released kinetics showed that the chitosan micro particles followed Higuchi model, which means the drug utilized the matrix system. Therefore, the chitosan microparticles were used to develop and modify the release of andrographolide.

5. CONCLUSION

The study showed that chitosan concentration from 0.5% to 0.75% affected entrapment efficiency. Its microparticles which were prepared by ionic gelation had the ability to enhance the andrographolide released by 2.0 times. Furthermore, the Higuchi's model was used to determine that the drug released from the chitosan matrix was based on diffusion. Therefore, the increase in the amount of chitosan from 0.5% to 0.75% caused a decrease in encapsulation with a release rate of andrographolide microparticles.

ACKNOWLEDGEMENT

-

REFERENCES

Agnihotri, S. A., Mallikarjuna, N. N. & Aminabhavi, T. M. 2004. Recent advances on chitosan-based micro- and nanoparticles. *Journal of Controlled Release* 100(1): 5-28.

Chellampillai, B. & Pawar, A.P. 2011. Improved bioavailability of orally administered andrographolide from ph-sensitive nanoparticles. *Drug metabolism pharmacokinetics* 35(3-4): 123–129.

He, P., Davis, S.S. & Illum, L. 1999. Chitosan microspheres prepared by spray drying. *International Journal of Pharmaceutics* 187(1): 53-65.

Hejjaji, E. M., Smith, A. M. & Morris, G. A. 2016. Designing chitosan-tripolyphosphate microparticles with desired size for specific pharmaceutical or forensic applications. *International Journal of Biological Macromolecules* 95: 564-573.

Jiang, Y., Wang, F., Xu, H., Liu, H., Meng, Q. & Liu, W. 2014. Development of andrographolide loaded plga microspheres: optimization, characterization and in vitro–in vivo correlation. *International Journal of Pharmaceutics* 475(1-2): 475–484.

Kanokwan, J. & Nubuo, N. 2008. Pharmacological aspects of andrographis paniculata on health and its major diterpenoid constituent andrographolide. *Journal of Health Science* 54(4): 370-381.

Ko, J.A., Park H.J., Hwang, S.J., Park, J.B. & Lee, J.S. 2002. Preparation and characterization of chitosan microparticles intended

for controlled drug delivery. *International Journal of Pharmaceutics* 249(1-2): 165-174.
Kumar, B.P., Chandiran, I.S., Bhavya, B. & Sindhuri, M. 2011. Microparticulate drug delivery system: A review. *Indian Journal of Pharmaceutical Science & Research* 1(1): 19-37.
Kumari, S., Nagpal, M., Aggarwal, G., Puneet, Jain, U.K. & Sharma, P. 2016. Microparticles drug delivery system: a review. *World Journal of Pharmacy and Pharmaceutical Sciences* 5(3): 543-566.
Malana, M.A., & Rubab Z. 2013. The release behavior abd kinetic evaluation of tramadol HCL from chemically cross linked ter polymeric hydrogel. *DARU Journal of Pharmaceutical Sciences* 21(1): 1-10.
Murphy, D.K. & Rabel, S. 2008. Thermal analysis and calorimetric methods for the characterization of new crystal forms. In: Adeyeye, M.C., Brittain, H.G (eds), *Preformulation in solid dosage form development*: 279-321. New York: Informa Healthcare USA, Inc.
Panossian, A., Hovhannisyan, A., Mamikonyan, G., Abrahamian, H., Hambardzumyan, E., Gabrielien, E., Goukasova, G., Wikman, G., & Wagner, H. 2011. Pharmacokinetic and oral bioavailability of andrographolid from andrographis paniculata fixed combination kan jang in rats and human. *Phytomedicine* 7(5): 351-364.
Rampino, A., Borgogna, M. & Blasi, P. 2013. Chitosan nanoparticles: preparation, size evalution and stability. *International Journal of Pharmaceutics* 455(1-2): 219-228.
Rasenack, N. & Müller, B.W. 2004. Micron-size drug particles: common and novel micronization techniques. *Pharmaceutical Development and Technology* 9(1): 1-13.
Rinaudo, M. 2006. Chitin and chitosan: properties and applications. *Progress in Polymer Science* 31(7): 603-632.
Sari., R., Soeratri, W. & Hendradi, E. 2017. Particulate delivery system of chitosan-diterpen lactone fraction of sambiloto (andrographis paniculata ness): preparation, characterization and in vitro drug release. *Asian Journal of Pharmaceutical and Clinical Research* 10(6): 175-179.
Sinha, V. R., Singla, A.K., Wadhawan, S., Kaushik, R., Kumria, R., Bansal, K. & Dhawan, S. 2004. Chitosan microspheres as a potential carrier for drugs. *International Journal of Pharmaceutics* 274(1–2): 1–33.
Sinko, P.J. & Yashveer S. 2011. *Martin's Physical Pharmacy and Pharmaceutical Sciences: Physical Chemical and Biopharmaceutical Principles in the Pharmaceutical Sciences*, 6th Edition. Philadelphia: Lippincott William & Wilkins.
Sonia, T.A. & Sharma, C.P. 2011. Chitosan and its derivatives for drug delivery perspective. In: *Chitosan for biomaterials I*: 24-49. New York: Springer.